Anthropomorphic physical breast phantom based on patient breast CT data: preliminary results

Sivo Daskalov[1], Nikiforos Okkaidis[2], J. M. Boone[3], Stoyko Marinov[4], Zhivko Bliznakov[4], Giovanni Mettivier[5], Hilde Bosmans[4], Paolo Russo[5], Kristina Bliznakova[1]

[1]Laboratory of Computer Simulations in Medicine, Technical University of Varna, Bulgaria
[2]Medical Physics Department, University of Malta, MSD2080, Malta
[3]Department of Radiology, University of California, Davis, Medical Center, Sacramento, CA, United States of America
[4]Department of Imaging and Pathology, KU Leuven, Herestraat 49, 3000 Leuven, Belgium
[5]Università di Napoli Federico II, Dipartimento di Fisica "Ettore Pancini", Via Cintia, I-80126 Napoli, Italy

csmlab@tu-varna.bg

Abstract. We propose a novel approach for the fabrication of realistic in shape, size as well as in x-ray absorption properties 3D physical breast models. The approach eliminates the need for segmentation of breast tissues by directly mimicking the radiodensity of each voxel in a computed tomography (CT) image. This is done through a recently published study that enables the use of variable filament extrusion rate when creating 3D phantoms with fused deposition modeling printers. We use the CT image of a real patient's breast to produce a model through the suggested approach. We then validate the fabricated physical breast phantom by obtaining a CT scan of it and comparing the latter to the original CT image of the source patient's breast.

Keywords:3D breast phantom fabrication, Fused deposition modeling, Variable filament extrusion rate

1 Introduction

Computer and physical anthropomorphic breast models have become a commonly utilized tool used in research for new breast imaging techniques[1], such as breast tomosynthesis, breast CT, and phase-contrast breast imaging. In literature relating to physical breast models, much effort has been devoted to the development of new 3D printing materials like photopolymers doped with different concentration of TiO_2, calcium, iodine and zinc. Other research has been directed towards the evaluation of available 3D printing materials such as ABS, different epoxy resin, nylon. A major challenge and requirement in the field of x-ray breast imaging is the use of materials exhibiting similar x-ray absorption coefficients to those of breast tissue, especially in the typical energy range used in mammography.

As a result, many works have been focused on measurements of the attenuation coefficients of various 3D printing materials used in the manufacturing of physical

breast phantoms. In the x-ray mammography range (between 22 kV and 32 kV), Carton *et al*[2] found that acrylic-based photopolymers are especially suitable to mimic the properties of the glandular breast tissue. Furthermore, Sikaria et al [3] and Zhao et al [4] doped the photopolymer materials with concentrations of the nanoscale TiO_2 and with calcium, iodine and zinc, with the aim to increase the the linear attenuation coefficients of the materials. From the tested ones, they found that zinc-doping can potentially increase attenuation to match and accurately mimic breast density.

Recently, we have studied the properties of available 3D printing materials with both stereolithography (SLA) and fuse deposition modeling (FDM) 3D printers [5]. This study concluded that most of the resins, Nylon, Hybrid, PET-G exhibit absorption properties close to glandular tissue, while ABS shows absorption characteristics similar to those of adipose tissue.

In a recent study, Okkaidis [6] showed that anthropomorphic physical phantoms can be fabricated without tissue segmentation from patient DICOM images through the use of an FDM printer by varying the infill density of some uniform infill pattern. The pattern is used to accurately mimic the internal structure of the modeled 3D object. The maximum infill density of 100% is used to produce the thickest parts of the object. Softer and lighter tissues are printed with a lower density, which results in miniature air pockets in the object.

Based on our study and the development of new approaches in printing anthropomorphic phantoms by Okkaidis [6] we explored the possible application of this new methodology to anthropomorphic breast model fabrication. The aim of this paper is to present the results of utilizing this novel approach in the preparation and manufacturing of realistic in shape and size 3D physical breast models.

2 Materials and methods

2.1 Overview

The main steps of the proposed approach for the creation of physical anthropomorphic breast phantoms are presented in Fig. 1. The main source of data is the computed tomography (CT) scans of real patient breasts [7, 8]. The novel modifiedFDM3D printing method proposed in [6] enables us to print voxels of varying radiodensity. This allows us to more realistically mimic the different types of tissue (glandular, adipose and skin) without requiring segmentation to be performed. The produced breast phantom is then scanned using CT and tomosynthesis. In order to validate the quality of the phantom, we use its CT scan to compare it to the CT scan of the original patient's breast and evaluate the similarities and differences.

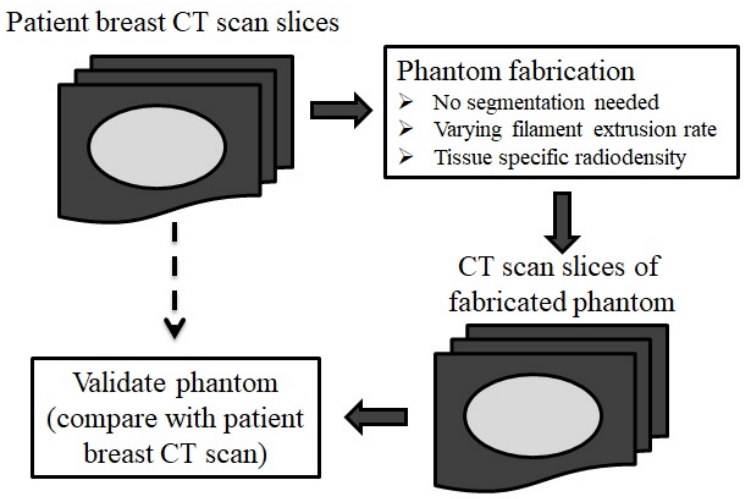

Fig. 1. Overview of the breast phantom creation and validation process.

2.2 Patient breast scanning

The patient's breast used as a source for the fabricated phantom is scanned using a Koning CT unit with tube voltage of 49 kVp. The unit's resolution of 672×656 pixels supports slice thickness and pixel size of 0.273 mm.

2.3 Phantom creation

Using a Fused Deposition Modeling (FDM) printer, patient-specific phantoms are normally fabricated by employing segmented 3D organ models. The phantoms are printed with a constant, estimated infill density which produces the required average Hounsfield Unit value for each organ. However, a recent method [6]demonstrated that it is possible to avoid long processing delays, such as manual contouring and 3D modeling, increase the achieved Hounsfield Units' range, and produce phantoms close to a specific patient's anatomy. This method involves the pixel-by-pixel printing by reading each Hounsfield Unit (HU) value in the DICOM image, and then controlling the filament extrusion rate to produce the required amount of extruded filament in the respective position in the phantom. This allowed us to fabricate the different types of tissues in the phantom more realistically in terms of radiodensity. The FDM printer used to produce the phantom was model T-Rex 2 (Formbot, China) with printing dimensions 400×400×470 mm. The filament, polylactic acid (PLA), was obtained from PrimaFilaments, Sweden.

2.4 Phantom scanning

Computed tomography images of the fabricated physical phantom were acquired with a Siemens unit featuring a detector with a resolution of 512 × 512 and pixel size of 0.85 × 0.85 mm. The tube voltage was 70 kVp. Two CT volumes were reconstructed with 1mm and 3mm, respectively. Additionally, the fabricated phantom was scanned with a GE Healthcare tomosynthesis unit. For this scan, both the anode and filter were molybdenum, and the source energy was 30 kVp.

3 Results and discussion

3.1 Fabricated breast phantom

An image of the fabricated physical breast phantom is shown on Fig. 2. The thickness of the phantom was 3 cm and the printing process took approximately 6 hours.

Fig. 2. Image of the fabricated physical phantom.

3.2 Phantom evaluation

The printed breast phantom was initially scanned at a tomosynthesis unit (Siemens Mammomat Inspiration). A slice from the reconstructed tomosynthesis volume of the fabricated phantom is shown in Fig. 3. As seen from this reconstructed slice, the air in

the printed phantom (used to decrease the density of the voxels) results in phase-contrast effects.

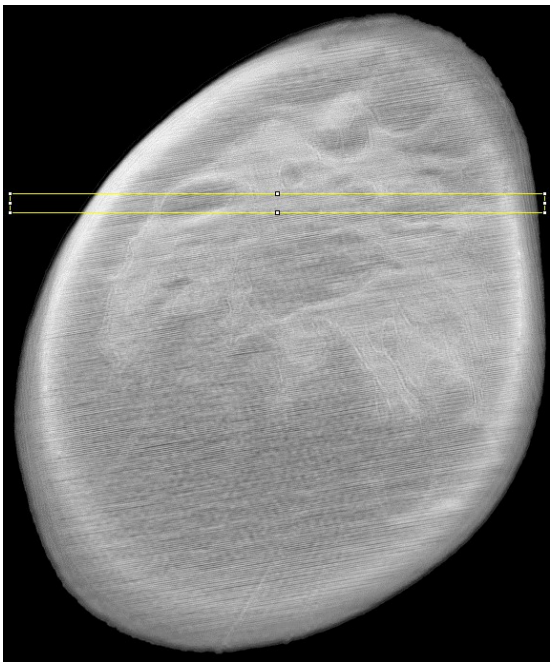

Fig. 3. Example tomosynthesis slice of the fabricated phantom

Side by side comparison of example CT scan slices is shown in Fig 4. The leftmost slice is of the source patient breast, while the following two are of the 1mm and 3mm CT scans of the fabricated phantom. The similarity between the original and the phantom's CT scan is clearly visible, especially the phantom scan with 3mm slices (C).

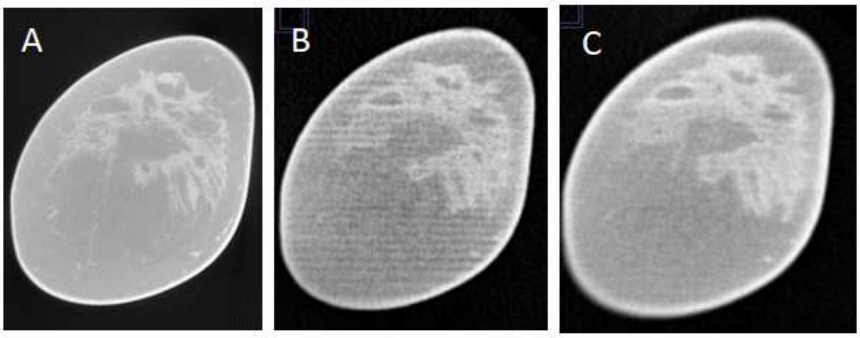

Fig. 4. Example CT slices. Left to right: patient breast (A), phantom 1mm (B) and 3mm (C).

We use the profile plotting functionality of *ImageJ* to visually verify the properties of the phantom. The function produces two-dimensional graphs of pixel intensities (column averaged) along a set of lines from the image. Fig. 5 shows the profiles of two subsets of 10 lines each chosen from the slices previously defined in Fig. 4.

The column-wise similarities are visibly significant, which validates the phantom fabrication procedure. In the context of computed tomography, the phantom (rows B and C) accurately models the various types of tissues present in the breast and may be considered to be a realistic representation of the source patient breast (row A).

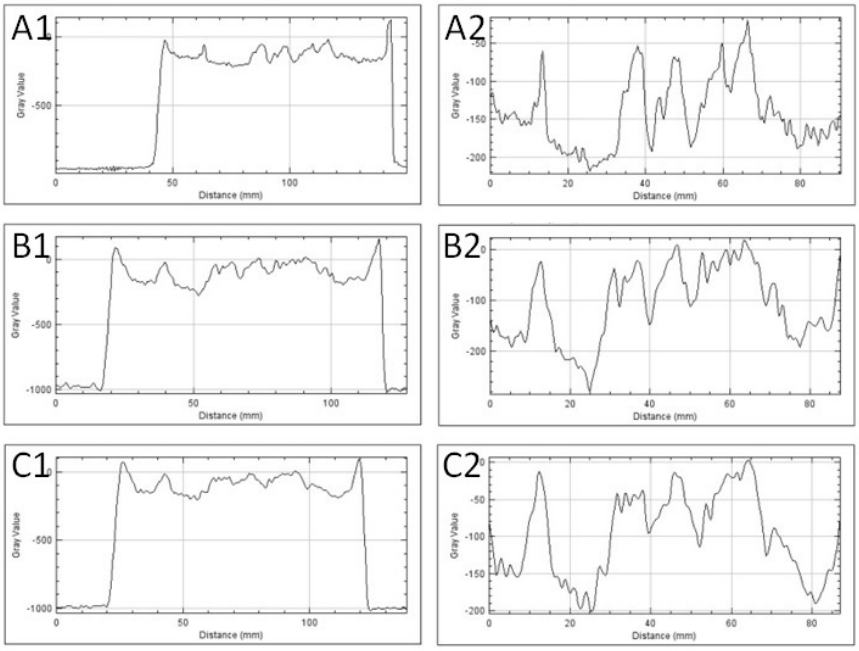

Fig. 5. ImageJ plot profiles of CT scan lines. The two columns result from the selection of two different subsets of 10 lines each. The rows correspond to the CT slices defined in Fig 4, namely A is the source patient breast, B and C are 1mm and 3mm slices of the phantom respectively.

In order to objectively verify the properties of the fabricated phantom numerically, we carried out the following evaluation and comparison procedure. The first step of the process was cropping the images along the respective object's (breast or phantom) bounding box. This was done to ensure uniform positioning in order to obtain more accurate results from the following steps. Then we extracted a vector of 64 features from each of the images through the use of KAZE [9], a 2D feature detection and description algorithm in nonlinear scale spaces. Finally, we compared the feature

vector from each image with all other feature vectors, using cosine similarity as a metric for the comparison. The final results from this statistical similarity evaluation are presented on the heatmap shown in Fig. 6.

The values of interest are the KAZE similarities between the real patient breast CT image (BCTNC16) and the CT images of the fabricated phantom, which are CT1MM and CT3MM respectively. Cosine similarity values of 0.58 for the 1mm slice CT and 0.65 for the 3mm slice CT are significant because no adjustment has been made to account for possible rotation or image resolution differences when scanning the fabricated phantom.

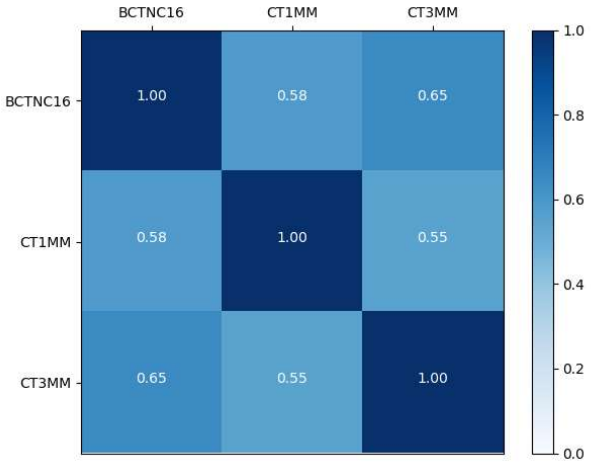

Fig. 6. Cosine similarity between the feature vectors of size 64 extracted from each image through the KAZE algorithm. Labels correspond to the CT slices defined in Fig 4, namely BCTNC16 is the patient breast, CT1MM and CT3MM are the 1mm and 3mm phantom slices

4 Conclusion

This paper presents the fabrication approach and initial results from tomosynthesis and CT imaging of an ad-hoc anthropomorphic breast phantom obtained with in-house developed 3D printer setup. Comparison of the CT images from the original patient and manufactured breast phantom showed similar visual appearance of the main breast tissues: adipose and gland, which is also well supported by the visual comparison of the *ImageJ* profiles taken across selected slices. Our numerical verification and evaluation procedure, comparing the KAZE feature vectors of the images, achieved promising results as well. Results of this study will be further exploited in the development of a dedicated phantom for breast CT studies and specifically in setting a future experimental setup for an accurate breast CT dosimetry study.

Acknowledgements:

This research is supported by the Bulgarian National Science Fund under grant agreement DN17/2.

References

1. S.J. Glick, L.C. Ikejimba, Advances in digital and physical anthropomorphic breast phantoms for x-ray imaging, Medical physics, 45 (2018) e870-e885.
2. A.K. Carton, P. Bakic, C. Ullberg, A.D.A. Maidment, Development of a 3D high-resolution physical anthropomorphic breast phantom, Medical Imaging 2010: Physics of Medical ImagingSan Diego, CA, 2010.
3. D. Sikaria, S. Musinksy, G.M. Sturgeon, J. Solomon, A. Diao, M.E. Gehm, E. Samei, S.J. Glick, J.Y. Lo, Second generation anthropomorphic physical phantom for mammography and DBT: Incorporating voxelized 3D printing and inkjet printing of iodinated lesion inserts, Medical Imaging 2016: Physics of Medical Imaging, 9783 (2016).
4. C. Zhao, J. Solomon, G.M. Sturgeon, M.E. Gehm, M. Catenacci, B.J. Wiley, E. Samei, J.Y. Lo, Third generation anthropomorphic physical phantom for mammography and DBT: Incorporating voxelized 3D printing and uniform chest wall QC region, Medical Imaging 2017: Physics of Medical Imaging, 10132 (2017).
5. D. Ivanov, K. Bliznakova, I. Buliev, P. Popov, G. Mettivier, P. Russo, F. Di Lillo, A. Sarno, J. Vignero, H. Bosmans, A. Bravin, Z. Bliznakov, Suitability of low density materials for 3D printing of physical breast phantoms, Phys Med Biol, 63 (2018).
6. N. Okkalidis, A novel 3D printing method for accurate anatomy replication in patient-specific phantoms, Medical physics, 45 (2018) 4600-4606.
7. J. Boone, Dedicated Breast CT Imaging of the Breast, Medical physics, 35 (2008).
8. K.K. Lindfors, J.M. Boone, T.R. Nelson, K. Yang, A.L.C. Kwan, D.F. Miller, Dedicated breast CT: Initial clinical experience, Radiology, 246 (2008) 725-733.
9. Alcantarilla P.F., Bartoli A., Davison A.J. (2012) KAZE Features. In: Fitzgibbon A., Lazebnik S., Perona P., Sato Y., Schmid C. (eds) Computer Vision – ECCV 2012. ECCV 2012. Lecture Notes in Computer Science, vol 7577. Springer, Berlin, Heidelberg